Cycling stability of a hybrid activated carbon//poly(3-methylthiophene) supercapacitor with N-butyl-Nmethylpyrrolidinium bis(trifluoromethanesulfonyl)imide ionic liquid as electrolyte

Andrea Balducci, Wesley Henderson, Marina Mastragostino, Stefano Passerini, Patrice Simon, Francesca Soavi

Cycling stability of a hybrid activated carbon//poly(3-methylthiophene) supercapacitor with *N*-butyl-*N*-methylpyrrolidinium bis(trifluoromethanesulfonyl)imide ionic liquid as electrolyte

Andrea Balducci, Wesley A. Henderson, Marina Mastragostino, Stefano Passerini, Patrice Simon and Francesca Soavi

UCI–Scienze Chimiche Radiochimiche e Metallurgiche, Università di Bologna, Via San Donato 15-40127 Bologna, Italy
CIRIMAT, UMR CNRS 5085, 118 Route de Narbonne, Toulouse Cedex 31062, France
ENEA (Italian National Agency for New Technologies, Energy and Environment), IDROCOMB, Casaccia Research Center, Via Anguillarese 301, 00060 Rome, Italy

Abstract

A long cycle-life, high-voltage supercapacitor featuring an activated carbon//poly(3-methylthiophene) hybrid configuration with *N*-butyl-*N*-methylpyrrolidinium bis(trifluoromethanesulfonyl)imide ionic liquid, a solvent-free green electrolyte, was developed. The cyclability of a laboratory scale cell with electrode mass loading sized for practical uses was tested at 60 °C over 16,000 galvanostatic charge–discharge cycles at 10 mA cm^{-2} in the 1.5 and 3.6 V voltage range. The reported average and maximum specific energy and power, specific capacitance and capacity, equivalent series resistance and coulombic efficiency over cycling demonstrate the long-term viability of this ionic liquid as green electrolyte for high-voltage hybrid supercapacitors.

Keywords: Hybrid supercapacitor; Ionic liquid; Poly(3-methylthiophene); Activated carbon; Cycle-life

1. Introduction
2. Experimental
3. Results and discussion
4. Conclusions
Acknowledgements
References

1. Introduction

The demand for clean energy is rapidly expanding worldwide and one of the most promising solutions proposed is non-polluting energy production by fuel cells. Supercapacitors, due to their capability to deliver high specific power during a few seconds or more, are presently considered as the electrical energy storage devices of choice for smoothing the strong and short-time power solicitations required in transportation and domestic applications powered by fuel cells or batteries, as well as for energy storage substations for voltage compensation in distributed networks [1], [2] and [3].

The most recent generation of supercapacitors on the market are double-layer carbon supercapacitors (DLCS), which make use of electrolyte solutions consisting of a salt dissolved in an aprotic organic solvent which permits relatively high operating voltages (about 2.5 V). The main drawback with these supercapacitors is that the organic solvents often do not fulfill the requirements of environmental compatibility and safety for vapor generation, flammability and explosions. This is the case for DLCSs with acetonitrile-based electrolytes, which are the most common high-voltage DLCSs on the market. The high vapor pressure of acetonitrile-based electrolytes requires a careful and expensive thermal control of the DLCSs when used in combination with fuel cells. Though DLCSs with liquid electrolytes based on propylene carbonate, a non-toxic and high boiling point solvent, are available, to further improve the safety and to increase the cell voltage of supercapacitors operating at high temperature, we pursued the strategy of using an ionic liquid (IL) as electrolyte in a supercapacitor featuring a recently developed hybrid configuration [4] and [5]. In such hybrid supercapacitor the negative and positive electrode materials are charged and discharged with different modes, electrostatic and Faradaic, which give rise to capacitive and pseudocapacitive electric responses, respectively.

ILs are salts that, as a result of unfavorable crystal packing, are often liquids at room and sub-ambient temperatures. The ionic nature of these materials and weak coordination

between the ions prevent their evaporation, so that these ILs have no measurable vapor pressure and a high chemical stability at high temperatures. Furthermore, ILs display wide electrochemical stability windows and good conductivities at the temperatures of interest for fuel cell coupling so that they can be used as solvent-free “green” electrolytes for high voltage supercapacitors [6], [7] and [8].

The use of ILs has been investigated both in DLCSs [9], [10] and [11] and in hybrid supercapacitors [4], but their cycling stability over a high number of cycles required by these power energy conversion systems is still to be proven. In the present paper, we report the results of cycling tests over more than 15,000 cycles for an activated carbon (AC)//poly(3-methylthiophene) (pMeT) hybrid supercapacitor with the *N*-butyl-*N*-methylpyrrolidinium bis(trifluoromethanesulfonyl)imide ($PYR_{14}TFSI$, Scheme 1) IL, operating at 60 °C and with an electrode mass loading suitable for practical applications. Among ILs, the $PYR_{14}TFSI$ [12] and [13] was selected mainly because of its appealing combination of properties, low melting temperature, hydrophobic nature, and high level of purity such as that required for long cycle-life, high-voltage supercapacitors.

Scheme 1. *N*-butyl-*N*-methylpyrrolidinium bis(trifluoromethanesulfonyl)imide ($PYR_{14}TFSI$).

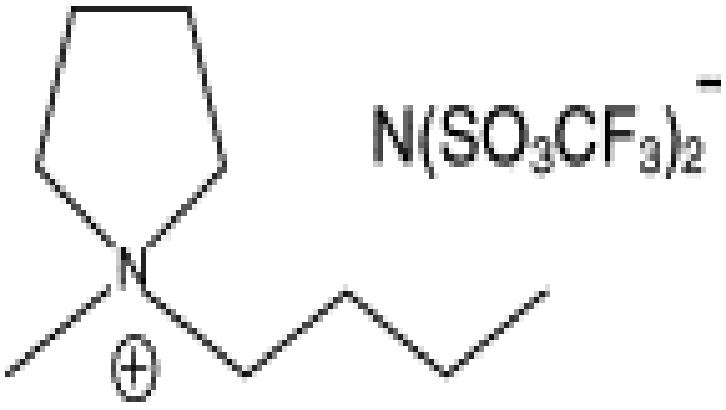

2. Experimental

$PYR_{14}TFSI$ was synthesized according to [13] from 1-methylpyrrolidine (97%) and 1-iodobutane (99%) (purchased from Aldrich and used as received) and LiTFSI (3 M). The $PYR_{14}TFSI$ was prepared by combining 1-methylpyrrolidine (Aldrich) with a stoichiometric amount of 1-iodobutane (Aldrich) in ethyl acetate. The resulting crystalline $PYR_{14}I$ was washed repeatedly using ethyl acetate until a pure white salt was obtained. The $PYR_{14}I$ was then dissolved in deionized water resulting in a clear, colorless solution. A stoichiometric amount of LiTFSI dissolved in deionized water was added and the mixture was stirred. The aqueous phase with dissolved LiI was removed and the remaining oily liquid was washed repeatedly with hot deionized water to purify the $PYR_{14}TFSI$ salt. The $PYR_{14}TFSI$ was dried under high vacuum (about 1 Pa) at 100 °C for 24 h and then 120 °C for 4–6 h. After purification and drying, the salt was a clear, colorless liquid at room temperature. The water content was lower than 20 ppm (Karl Fisher titration, 684 KF Coulometer Metrohm). The material was stored and handled in a dry room (<0.2% RH, 20 °C) or a dry box (MBraun Labmaster 130).

Thermogravimetric measurements (TGA) were carried out with a Mettler Toledo STAR^e System in the temperature range 25–600 °C under N_2 flow with a scanning rate of 20 °C min^{-1}. An alumina pan with lid was used.

Conductivity measurements were carried out with a AMEL mod.160 conductivity-meter. The cell was thermally equilibrated in a Haake thermocryostat at each temperature for at least 4 h before measurements that were taken on the heating cycle.

Evaluation of the electrochemical stability window was carried out by linear sweep voltammetry (LSV) at 5 mV s^{-1} in dry box with Pt working electrode, carbon paper counter electrode, and Ag quasi-reference electrode whose potential was measured by adding the highly reversible redox couple ferrocene/ferrocinium (Fc/Fc^+) to the medium (at 60 °C, $E_{1/2,Fc/Fc^+}$=432 mV versus saturated calomel electrode, E_{Ag} = −220 mV versus $E_{1/2,Fc/Fc^+}$).

The pMeT and AC electrodes were composite materials prepared by mixing 80% (w/w) pMeT (Polyscience, as received) and 15% (w/w) acetylene black (AB, Hoechst), or 95% (w/w) AC (PICACTIF Supercap BP, BET specific surface area >2000 m^2 g^{-1}, dried in Büchi oven under dynamic vacuum of a rotary pump at 120 °C for 12 h) with 5% (w/w)

polytetrafluoroethylene binder (PTFE, Du-Pont). The mixtures were laminated on Al/C grid current collectors (Lamart) and the AC and pMeT composite electrodes were dried under dynamic vacuum for 12h at 120 and 60 °C, respectively. Supercapacitors were prepared by facing two AC and pMeT composite electrodes of geometric area of 0.25 cm^2, with single electrode mass loading in the range from 4 to 8 mg cm^{-2} of geometric area, with a spacing of about 0.5 mm. Such a high spacing was required because common separators used in liquid organic electrolyte supercapacitors (such as that used in ref. [5]) did not perform well with the $PYR_{14}TFSI$ IL. Prior to assembling the supercapacitors, the electrodes were separately activated by cycling several dozen times at 20 mV s^{-1} in the operating potential ranges of the positive and negative electrodes: the pMeT was first activated in propylene carbonate (PC, distilled, Fluka)-1 M LiTFSI (3 M, dried before use) at room temperature and then in $PYR_{14}TFSI$ at 60 °C; the AC electrode was directly activated at 60 °C in $PYR_{14}TFSI$. The supercapacitors were assembled and characterized in dry box and were kept at the controlled temperature of 60 ± 2 °C by a Thermoblock (FALC).

Electrochemical tests were performed with a Perkin-Elmer VMP multichannel potentiostat/galvanostat. Quasi-reference Ag wire electrodes were used to check the electrode potentials upon the voltammetric activations and the supercapacitor galvanostatic cycles.

3. Results and discussion

Before supercapacitor assembly, we carried out some characterizations of the $PYR_{14}TFSI$ that we prepared. The TGA trace reported in Fig. 1, shows a weight loss lower than 0.1% up to 360 °C, evidences the thermal stability and the high level of purity of this IL. In Fig. 2, the Arrhenius conductivity plot of the $PYR_{14}TFSI$ in the temperature range from 20 °C to 80 °C shows that at temperatures of 60 °C or higher, which are of interest for fuel cell and supercapacitor coupling, the conductivity (σ) of $PYR_{14}TFSI$ is comparable to that of many conventional liquid organic electrolytes based on tetraalkylammonium salts, hence we selected 60 °C as operating temperature of the AC/IL/pMeT hybrid supercapacitor. In order to investigate the anodic and the cathodic $PYR_{14}TFSI$ stability window at such temperature, we carried out LSVs with a Pt electrode at 60 °C and the curves are reported in Fig. 3. The anodic and cathodic currents may correspond to the oxidation of the $TFSI^-$ anion and the reduction of the PYR_{14}^+ cation, respectively. The $PYR_{14}TFSI$ displays an overall maximum stability window of 6 V as evaluated from the potentials corresponding to cathodic and anodic currents

of 1 mA cm^{-2}, an interesting value especially when compared to the lower values of PC-based electrolytes at the same temperature.

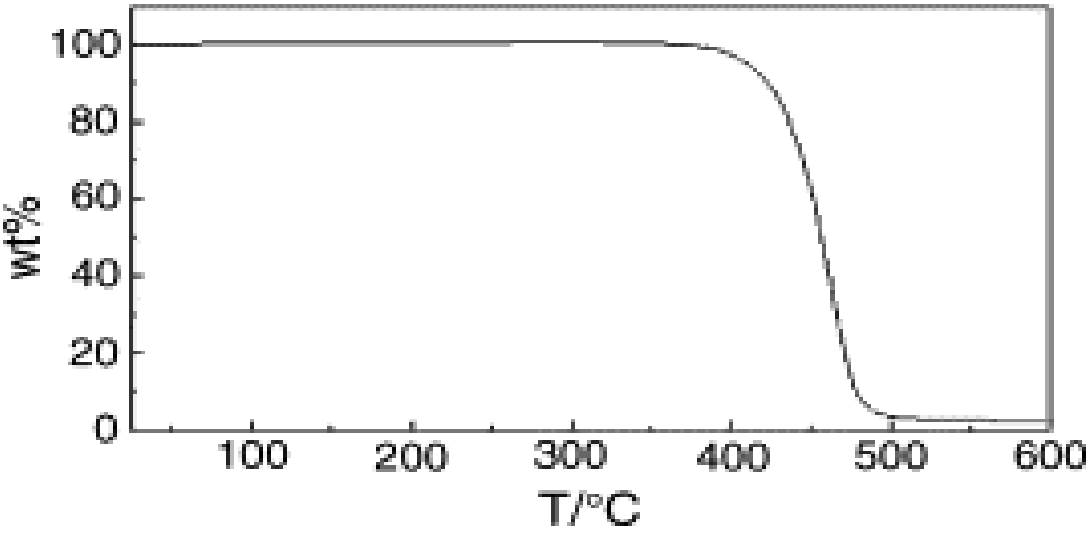

Fig. 1. TGA heating trace of $PYR_{14}TFSI$.

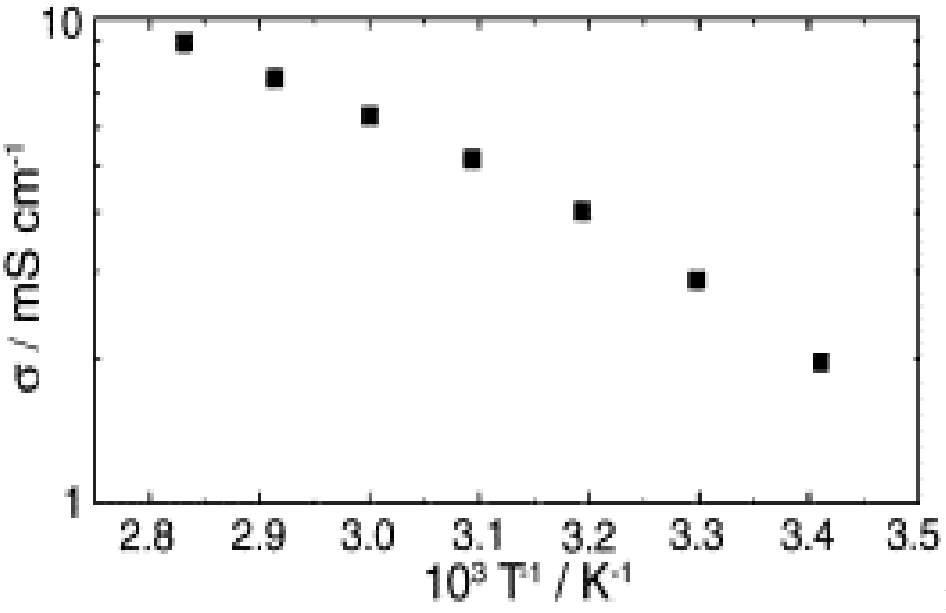

Fig. 2. Arrhenius conductivity plot of $PYR_{14}TFSI$ from 20 °C up to 80 °C.

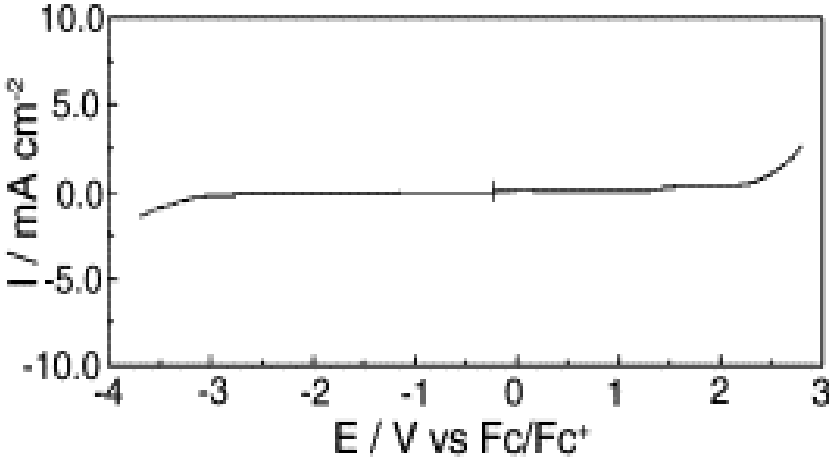

Fig. 3. LSVs of $PYR_{14}TFSI$ with Pt electrode at 5 mV s^{-1} and 60 °C.

Fig. 4 reports the specific capacitances of the AC and pMeT electrodes in Farad per gram of active material (C_{am}), as estimated from cyclic voltammetry (CV) at 20 mV s^{-1} and 60 °C in $PYR_{14}TFSI$. Average values of about 50 and 100 F g^{-1} were obtained for the AC and pMeT electrodes, respectively, by the slope of the plots integrated current over time (upon CV discharge) versus electrode potential. These values are substantially lower (about 50%) than those obtained with the same AC and electrochemically synthesized pMeT electrodes in PC-tetraethylammonium tetrafluoroborate electrolyte [5] and clearly indicate the need to optimize the electrode morphology as well as the active material's affinity toward the hydrophobic IL.

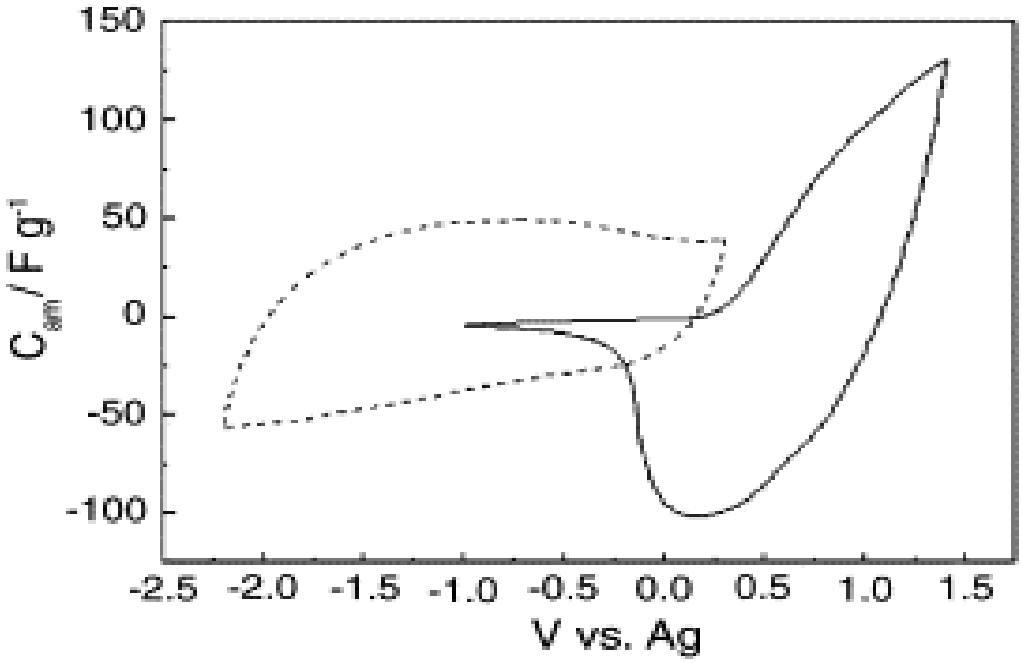

Fig. 4. C_{am} values vs. voltage of the AC negative electrode (dashed line) and the pMeT positive electrode (straight line) in $PYR_{14}TFSI$ electrolyte at 60 °C as obtained from CV at 20 mV s^{-1} by dividing specific current per scan rate.

On the basis of the capacitance values obtained from the tests on the single electrodes in $PYR_{14}TFSI$ and to limit the end-of-charge voltage of the negative and positive electrodes in a safe potential range, i.e. −2.2/+1.6 V versus Ag which ensures coulombic efficiency for their charge–discharge processes higher than 95%, and for a maximum operating voltage of 3.6 V, a AC/$PYR_{14}TFSI$/pMeT hybrid supercapacitor was prepared with the electrode-active mass loading ratio pMeT/AC of 0.42. The total mass of the two composite electrode materials w_{tcm} was 12 mg cm^{-2}. The device was tested by charge–discharge galvanostatic cycles at 60 °C over 16,000 cycles at 10 mA cm^{-2} between 1.5 and 3.6 V. Fig. 5 shows the supercapacitor voltage profile at the 1000th galvanostatic cycle, as well as the voltage profile of each electrode vs. Ag. For the 1000th cycle, the supercapacitor delivered a specific capacity (Q_{tcm}) of 6.1 mA h/g of the composite electrodes (the weight of both electrodes is included in the calculation) with a coulombic efficiency of 99.3%. From the supercapacitor voltage profile a capacitance of 0.18 F cm^{-2} is calculated, which corresponds to a capacitance per gram of total composite electrode materials (C_{tcm}) of 15 F g^{-1}. The equivalent series resistance (ESR, in Ω cm^2) calculated from the ohmic drop at the beginning of the discharge

was 17 Ω cm^2. Such a high value, which is importantly affected by the bulk electrolyte resistance (ca. 8 Ω cm^2) as a result of the large distance between the two electrodes (about 0.5 mm), substantially reduced the effective full-charge voltage V_{max} (i.e. the charge cut-off voltage minus the ohmic drop) to only 3.43 V. The average specific energy, E_{av}, and power, P_{av}, delivered upon discharge from 3.43 V down to 1.5 V, were 14 W h kg^{-1} and 1.9 kW kg^{-1}, respectively, as evaluated by Eqs. (1) and (2)

$$E_{av} = i\int_{t}^{t+\Delta t} \frac{V\,dt}{w_{tcm}} \quad ((1)) \quad (1)$$

and

$$P_{av} = \frac{E_{av}}{\Delta t}, \quad ((2)) \quad (2)$$

where i is the current density, V the cell potential and Δt the discharge time. The maximum specific energy, E_{max}, and power, P_{max}, were 24 W h kg^{-1} and 14 kW kg^{-1}, respectively, as evaluated by Eqs. (3) and (4)

$$E_{max} = \tfrac{1}{2} C_{tcm} V_{max}^2 \quad ((3)) \quad (3)$$

and

$$P_{max} = \frac{V_{max}^2}{4ESR w_{tcm}}. \quad ((4)) \quad (4)$$

The energy and power performance of the AC/PYR_{14}TFSI/pMeT hybrid supercapacitor upon cycling are very promising, particularly considering the non-optimized cell design and components, as shown in Fig. 6, that reports the trend of the average specific energy and power, maximum specific energy and power, specific capacitance, ESR, specific capacity and coulombic efficiency upon long-term cycling (the first thousand cycles are not reported because they are not representative of the supercapacitor functioning). At the 16,000th cycle the supercapacitor was able to deliver 90% of the initial average specific power. To our knowledge, this is the first report concerning the long-term viability of IL-based, hybrid supercapacitors. The average specific energy and the maximum specific energy and power are, at the 16,000th cycle, about 40–50% of the initial values as a result of the capacitance decrease and the ESR increase mainly caused by a decrease of the positive electrode performance. The non-optimized mass balancing of the electrode materials in the supercapacitor pushes the positive electrode to operate at high potentials that are detrimental for the pMeT stability as evidenced by a lowering of the coulombic efficiency, which is only 97.5% at the 16,000th cycle, and by the increase of the electrode resistance. Also, the increase of the ESR might result from a deterioration of the electrode material/current collector contact at both the positive and negative electrodes, most likely due to the ability of the IL used (PYR_{14}TFSI) to slightly swell the binder of the composite electrodes. The device components used in this initial work were optimized for electrolytes containing organic “molecular” solvents [5] and not for the hydrophobic, room temperature ILs. Nevertheless, after 16,000 cycles the AC/PYR_{14}TFSI/pMeT hybrid supercapacitor delivered specific energy and power that are of practical interest thus demonstrating the viability of the use of ILs in such devices.

For example, if the initial ESR would be lowered to about 10 Ω cm^2 (via an optimized separator that would reduce the electrode spacing) and by considering the same trend reported in Fig. 6, after 16,000 cycles the maximum specific energy and power would become approximately 12 W h kg^{-1} and 13 kW kg^{-1}, respectively.

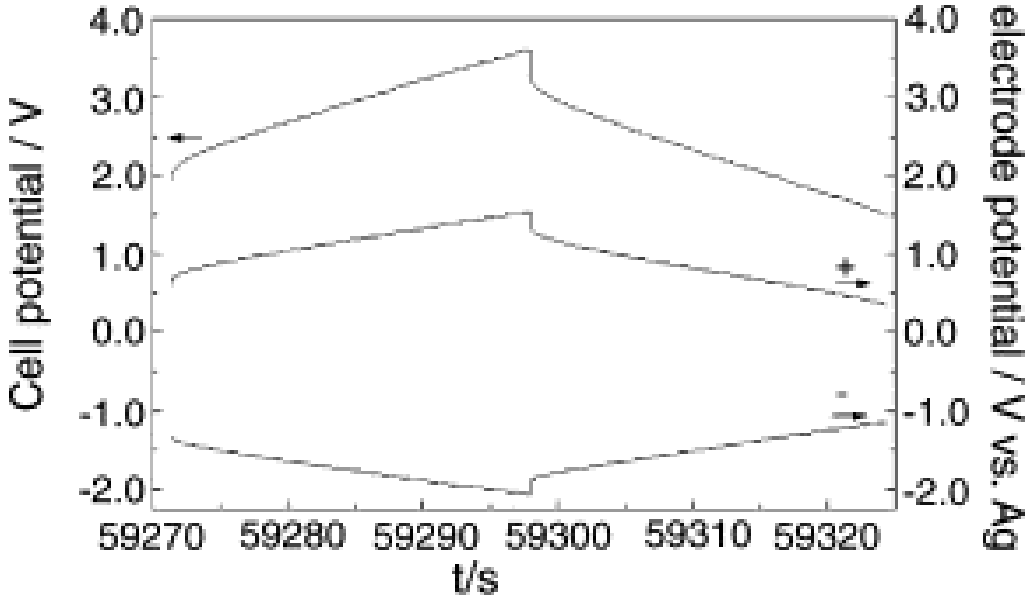

Fig. 5. Voltage profile of the AC/PYR_{14}TFSI/pMeT hybrid supercapacitor and its positive and negative electrodes during the 1000th galvanostatic cycle at 10 mA cm^{-2} and 60 °C.

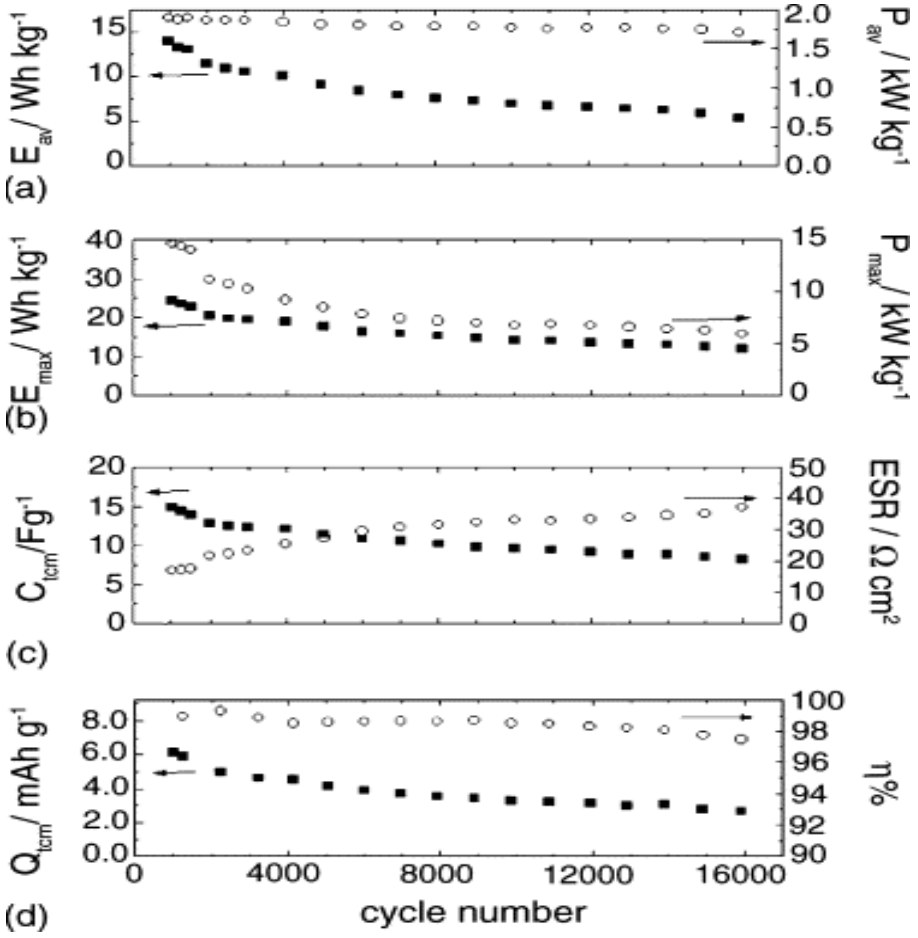

Fig. 6. Trend vs. cycle number of the (a) average specific energy and power, (b) maximum specific energy and power, (c) specific capacitance and ESR and (d) specific capacity and coulombic efficiency of the AC/PYR_{14}TFSI/pMeT hybrid supercapacitor from galvanostatic cycles at 10 mA cm^{-2} with a 3.6–1.5 V cell cut-off at 60 °C.

4. Conclusions

To our knowledge, this is the first report describing the long-term viability of ILs as solvent-free (green) electrolytes for high-voltage hybrid supercapacitors. The device prepared in this work showed good performance during prolonged cycling tests (several thousand cycles) at a temperature required for direct fuel-cell coupling. After the first thousand cycles at 10 mA cm^{-2} and 60 °C (voltage cut-off 3.6–1.5 V), the AC/PYR_{14}TFSI/pMeT hybrid supercapacitor delivered 24 W h kg^{-1} and 14 kW kg^{-1} as maximum values. Work is in progress to enhance the specific energy and power by optimizing the entire system including

the reduction of the ESR by the search for a suitable separator and binder, and by selecting electrode materials (especially the activated carbon) showing higher affinity for the hydrophobic IL. Optimization of the electrode mass balancing is also expected to enhance the overall performance of the system.

Acknowledgments

We wish to thank the Italian–French University for providing a Ph.D. grant to Andrea Balducci as part of the Vinci Project 2003, involving Paul Sabatier University of Toulouse (France) and Bologna University (Italy), and INSTM for Francesca Soavi's postdoctoral research contract. Wesley A. Henderson is indebted to the National Science Foundation for the award of a fellowship (International Research Fellowship Program 0202620).

References

M. Mastragostino, C. Arbizzani and F. Soavi In: W.A. Van Schalkwijk and B. Scrosati, Editors, *Advances in Lithium-Ion Batteries,* Kluwer Academic Publishers/Plenum Press, New York (2002) (Chapter 16).

R.J. Brodd, K.R. Bullock, R.A. Leising, R.L. Middaugh, J.R. Miller and E. Takeuchi, *J. Electrochem. Soc.* 151 (2004), p. K1.

A. Rufer, *IEEE Trans. Power Delivery* 19 (2004), p. 629.

A. Balducci, U. Bardi, S. Caporali, M. Mastragostino and F. Soavi, *Electrochem. Commun.* 6 (2004), p. 566.

A. Laforgue, P. Simon, J.F. Fauvarque, M. Mastragostino, F. Soavi, J.F. Sarrau, P. Lailler, M. Conte, E. Rossi and S. Saguatti, *J. Electrochem. Soc.* 150 (2003), p. A645.

C. Nanjundiah, S.F. McDevitt and V.R. Koch, *J. Electrochem. Soc.* 144 (1997), p. 3392.

A.B. McEwen, H.L. Ngo, K. Le Compte and J.L. Goldman, *J. Electrochem. Soc.* 146 (1999), p. 1687.

D. Adam, *Nature* 407 (2000), p. 938.

A. Lewandowski and A. Swiderska, *Solid State Ionics* 161 (2003), p. 243.

M. Ue, M. Takeda, A. Toriumi, A. Kominato, R. Hagiwara and Y. Ito, *J. Electrochem. Soc.* 150 (2003), p. A499.

A. Lewandowski and M. Galinski, *J. Phys. Chem. Solids* 65 (2004), p. 281.

D.R. MacFarlane, P. Meakin, J. Sun, N. Amini and M. Forsyth, *J. Phys. Chem. B* 103 (1999), p. 4164.

W.A. Henderson and S. Passerini, *Chem. Mater.* 16 (2004), p. 2881.

Corresponding author. Tel.: + 39 051 2099798; fax: +39 051 2099365.
ISE member.